



PHONON ENERGY REMOVAL FROM HIGH-POWER ACOUSTO-OPTIC DEVICES

Vladimir Molchanov^{1*}

Konstantin Yushkov¹
Sergey Tretiakov³

Alexander Darinskii^{1,2}

¹ Acousto-Optical Research Center, University MISIS, Russia

² Institute of Crystallography FSRC “Crystallography and Photonics,” Russia

³ Tver State University, Russia

ABSTRACT

We study active BAW energy removal by a piezoelectric receiver from high-power-consuming acousto-optic devices for infrared photonics. The piezoelectric receiver converts the ultrasonic wave into an electrical signal, which is dissipated in an external electrical load. It is analytically shown that in the plane wave approximation BAW reflection from the receiver tends to zero at a certain choice of complex load or at the 50 Ohm active load transformed by the matching circuit to the optimal complex value.

Theoretical calculations are confirmed by experiments. We designed and fabricated a SiO₂-based custom acoustic device with two LN transducers, an emitter and a receiver, corresponding to a typical geometry of acousto-optic interaction in the laser Q-switches. Experimental measurements demonstrated that over 60 % of the incoming into device RF power in the operating bandwidth of 21–28 MHz could be removed by the receiver from the SiO₂ crystal into the external electrical load.

Keywords: *acousto-optics, laser Q-switch, piezoelectric transducer, thermal stabilization, matching circuit.*

1. INTRODUCTION

Among the acousto-optic (AO) devices for controlling laser radiation [1, 2], a special place is occupied by AO

Q-switches for solid-state lasers operating in the giant pulse generation mode. As a rule, fused and crystalline quartz SiO₂ is used in the Q-switches. Quartz has a high laser-induced damage threshold but is characterized by a low AO figure of merit M_2 , which determines the control RF power of the Q-switch [1–3]. A typical AO laser Q-switch based on quartz at a wavelength of 1.064 μm consumes RF power of the order of 30 Watts. Usually, either water cooling or thermoelectric elements are used. A feature of all AO devices is the quadratic dependence of the diffraction efficiency on the laser wavelength [1–3]. For example, when operating in a pulsed holmium laser based on Ho³⁺:YAG, 2.1 μm [4, 5], to achieve the same level of efficiency as at the wavelength of 1.064 μm, all other things being equal, a control RF power of the order of 120 W is theoretically required, which will lead to the destruction of the device. This fundamental feature of AO interaction is a serious limiting factor in the use of new high-power mid-IR lasers of 2–5 μm wavelength region. Currently, mid-IR lasers are being intensively developed. Most of them operate in a pulsed mode, but electro-optical shutters, passive shutters based on liquids or crystals, for example, on Fe²⁺:ZnSe, and even mechanical ones are used as Q-switches [6, 7]. Thus, development of AO Q-switches is a challenge for improvement laser efficiency in the mid-IR range, for example: Cr²⁺:CdSe for 2.26–3.61 μm [8]; Fe²⁺:ZnS for 3.49–4.65 μm [9]; Fe:ZnSe for 4.0–4.5 μm [10]; femtosecond laser systems with amplifiers based on Fe²⁺:ZnSe for 4–5 μm [11], Cr:ZnS and Cr:ZnSe polycrystals for 1.9–3.4 μm, and Fe:ZnS and Fe:ZnSe polycrystals for 3.4–5 μm [12].

*Corresponding author: aocenter@misis.ru

Copyright: ©2023 Vladimir Molchanov et al. This is an open-access article distributed under the terms of the Creative Commons Attribution 3.0 Unported License, which permits unrestricted use, distribution, and reproduction in any medium, provided the original author and source are credited.



2. THE CONCEPT OF REMOVING PHONON ENERGY FROM AN AO CRYSTAL

In any AO device, there are two main principal heat sources in an AO crystal: a piezoelectric transducer and a dissipative absorber of bulk acoustic waves (BAW) after diffraction, which provides the traveling BAW mode in the AO device. Bulk acoustic absorption in the AO laser Q-switch crystals can be neglected, since they operate at relatively low frequencies of 25–50 MHz. The heating of the entire crystal due to the dissipation of acoustic energy is significant if there is no damper.

If the piezoelectric transducer has low losses for converting electrical energy into acoustic energy, say 1.5–2.0 dB, its contribution to the heating of the AO crystal is not decisive. A significant factor is the heating from the acoustic damper, since it absorbs the bulk of the BAW energy. Many types of acoustic dampers for AO devices are known from the literature. However, fundamentally they are all of the dissipative type.

The dissipative acoustic power absorber in the AO device is structurally always located on the AO crystal and heats it. If a method for actively transferring or extracting the BAW energy from the crystal were found, then the problem of reducing the temperature of the AO Q-switch and increasing the stability of the laser in the mid-IR range would be solved to a certain extent.

In this paper, for the first time, an original method is theoretically proposed and experimentally confirmed: replacing a conventional dissipative damper with an active device that transforms the energy of acoustic waves into electrical energy and removes it via an RF cable to a matched electrical load. This method is based on the conversion of acoustic energy through the use of a second, receiving, piezoelectric transducer in the AO device. If a significant part of the acoustic energy could be removed from the AO crystal, then it became possible to extend the use of AO laser Q-switch to the mid-IR range, where they are practically not used now. Besides that, a recently developed new type of AO laser Q-switch based on low-symmetry $KRe(WO_4)_2$ crystal family and first used in lasers in the 2.0–3.0 μm range [13, 14] could be extended further into the IR region.

3. THEORETICAL ANALYSIS OF BAW ABSORPTION BY A PIEZOELECTRIC RECEIVER

The proposed method for reducing the reflection coefficient of an acoustic wave from the crystal boundary involves the creation of a crystal-plate

structure, where a piezoelectric plate with metallized surfaces is attached to one of the crystal facets so that acoustic contact is provided between the plate and the crystal (Fig. 1a). The mechanical vibrations of a piezoelectric plate, as well as the transmission of acoustic waves through a set of layers that provide contact between the piezoelectric plate and the crystal, will be described by the transfer matrix method [15–17]. In our work, the transfer matrix method will allow us to derive an analytical expression for the reflection coefficient of an acoustic wave incident from the crystal onto the “layered structure + piezoelectric plate” system, and then obtain analytical expressions for the parameters of an external matching electrical circuit connected to the piezoelectric plate, at which the coefficient reflection vanishes almost in a certain frequency band (Fig. 1b). We assume that there is a bonding layered structure between the transducer and the crystal, which provides good acoustic contact (Fig. 1a).

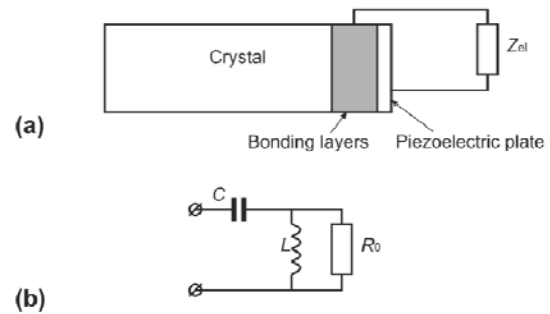


Figure 1. a) Crystal, piezoelectric transducer and bonding layers; b) Complex electrical load. Active resistance $R_0=50$ Ohm is the matched electrical load.

A piezoelectric plate is described by a transfer matrix

$$\hat{m} = \begin{pmatrix} m_{11} & m_{12} \\ m_{21} & m_{11} \end{pmatrix}, \quad (1)$$

where

$$\begin{aligned} m_{11} &= M_{11} - \frac{M_{14}M_{21}}{i\omega SZ_{el} + M_{24}}, & m_{12} &= M_{13} - \frac{M_{14}^2}{i\omega SZ_{el} + M_{24}}, \\ m_{21} &= M_{31} - \frac{M_{21}^2}{i\omega SZ_{el} + M_{24}}, & M_{11} &= \cos\left(\frac{\omega}{v}d\right), \\ M_{13} &= \frac{1}{\omega Z} \sin\left(\frac{\omega}{v}d\right), & M_{14} &= \frac{e}{\epsilon\omega Z} \sin\left(\frac{\omega}{v}d\right), \\ M_{21} &= \frac{e}{\epsilon} \left[\cos\left(\frac{\omega}{v}d\right) - 1 \right], & M_{31} &= -\omega Z \sin\left(\frac{\omega}{v}d\right), \\ M_{24} &= \frac{e^2}{\epsilon^2\omega Z} \sin\left(\frac{\omega}{v}d\right) - \frac{d}{\epsilon}, \end{aligned}$$

v is the speed of sound in the plate, $Z = \rho v$ is the mechanical impedance of the plate, ρ is the density, e is the piezoelectric modulus, ϵ is the permittivity, S is the area of the plate, Z_{el} is the load electrical impedance. Each of the layers of the binding structure is characterized by a transfer matrix similar to (1), but having $M_{14} = M_{21} = 0$, since the layers are not piezoelectric.

It can be shown that the expression for the reflection coefficient R has the form:

$$R = \frac{n_{21} + i\omega n_{22} Z_c}{i\omega n_{22} Z_c - n_{21}}, \quad (2)$$

where n_{21} and n_{22} are matrix elements

$$\hat{n} = \hat{m}\hat{m}' = \begin{pmatrix} n_{11} & n_{12} \\ n_{21} & n_{22} \end{pmatrix}, \quad (3)$$

\hat{m}' is the transfer matrix of the binding structure as a whole. In particular,

$$\begin{aligned} n_{21} &= m_{21}m'_{11} + m_{11}m'_{21} = N_{21} - \frac{N_{p21}}{i\omega S Z_{el} + M_{24}}, \\ n_{22} &= m_{21}m'_{12} + m_{11}m'_{22} = N_{22} - \frac{N_{p22}}{i\omega S Z_{el} + M_{24}}, \end{aligned} \quad (4)$$

where

$$\begin{aligned} N_{21} &= M_{31}m'_{11} + M_{11}m'_{21}, \\ N_{p21} &= (M_{21}m'_{11} + M_{14}m'_{21})M_{21} \\ N_{22} &= M_{31}m'_{12} + M_{11}m'_{22}, \\ N_{p22} &= (M_{21}m'_{12} + M_{14}m'_{22})M_{21}. \end{aligned} \quad (5)$$

The reflection coefficient R vanishes at the frequency ω_0 provided that the impedance of the external electrical circuit (Fig. 1b) is equal to

$$Z_{el}^{(0)} = \frac{1}{i\omega_0 S} \left(\frac{N_{p21} + i\omega_0 N_{p22} Z_c}{N_{21} + i\omega_0 N_{22} Z_c} - M_{24} \right). \quad (6)$$

The impedances X_l and X_c of the inductor and capacitor, respectively, at which the total impedance is $Z_{el}^{(0)}$ (6), are

$$X_l = \sqrt{\frac{R_0^2 \operatorname{Re}(Z_{el}^{(0)})}{R_0 - \operatorname{Re}(Z_{el}^{(0)})}}, X_c = \operatorname{Im}(Z_{el}^{(0)}) + \frac{R_0^2 X_l}{R_0^2 + X_l^2}, \quad (7)$$

and then

$$L_0 = X_l / \omega_0, C_0 = \omega_0 / X_c. \quad (8)$$

Therefore, the frequency dependence of the impedance included in the plate transfer matrix elements is described by the expression

$$Z_{el}(\omega) = \frac{i}{\omega C_0} - \frac{iR_0 \omega L_0}{R_0 - i\omega L_0}. \quad (9)$$

Let us consider the typical design parameters of an AO laser Q-switch for unpolarized radiation based on SiO₂ crystal [19]. Longitudinal piezoelectric plate is lithium niobate (LN) Y+36° with an area of $S=2.5 \times 27 \text{ mm}^2$ with $K_p=0.49$, $\rho_p=4700 \text{ kg/m}^3$, $\epsilon_p=4.04 \times 10^{-10} \text{ F/m}$. Resonance frequency $f_R=50 \text{ MHz}$. A longitudinal wave propagates in a crystal along X axis. The phase velocity is $v_c=(c_{11}/\rho)^{1/2}$, where $c_{11}=8.67 \times 10^{10} \text{ N/m}^2$, $\rho=2648 \text{ kg/m}^3$. The directions of the phase and group velocities coincide.

The binding structure is determined by the manufacturing technology and in our case contains 5 layers [3],

$$\text{Cr (0.05 } \mu\text{m)} - \text{Au (0.15 } \mu\text{m)} - \text{In (0.4 } \mu\text{m)} \\ - \text{Au (0.15 } \mu\text{m)} - \text{Cr (0.05 } \mu\text{m)} \quad (10)$$

with material constants

$$\text{Cr: } c_{11} = 15.08 \cdot 10^{10} \text{ N/m}^2, \rho = 7190 \text{ kg/m}^3;$$

$$\text{Au: } c_{11} = 12.52 \cdot 10^{10} \text{ N/m}^2, \rho = 19300 \text{ kg/m}^3; \quad (11)$$

$$\text{In: } c_{11} = 4.85 \cdot 10^{10} \text{ N/m}^2, \rho = 7310 \text{ kg/m}^3;$$

Note that the material constants in thin metal layers may differ from those known for bulk samples [20, 21].

4. CALCULATION RESULTS

Figure 2 shows 4 cases of the BAW reflection coefficient $|R|$ from the piezoelectric receiver depending on the frequency of the BAW and the parameters of the matching circuit. In all cases, the "zero" frequency is equal to $f_0=f_R$.

Line 1 is calculated taking into account the presence of bonding layers, i.e., R is found from (2) and $Z_{el}(\omega)$ is given by (9), where L_0 and C_0 are calculated from (6) and (7), namely

$$L_0 = 57.7 \text{ nH}, C_0 = 480.1 \text{ pF}. \quad (12)$$

Line 2 is obtained when bonding layers are not taken into account. Then, $\hat{n} = \hat{m}$, and from the correspondingly simplified expression (6) we determine $Z_{el}^{(0)}$, and then we find from relations (7) the inductance and capacitance,

$$L'_0 = 58.6 \text{ nH}, C'_0 = 416.8 \text{ pF.} \quad (13)$$

and the impedance $Z_e(\omega)$ in the expression for R is calculated according to (9), where L_0 and C_0 are replaced by L'_0 and C'_0 (13), respectively. Line 3 is calculated using (2), but $Z_e(\omega)$ is found from (9), where we substitute L'_0 and C'_0 (13), i.e., the inductance and capacitance values are used, calculated without taking into account the coupling layers. Line 4 is calculated following (2), and $Z_e(\omega)$ is found from (9), where C_0 is substituted, and L_0 is replaced by $L=1.1L_0$. Note that in the case under consideration, L_0 and L'_0 are quite close, while C_0 and C'_0 differ significantly.

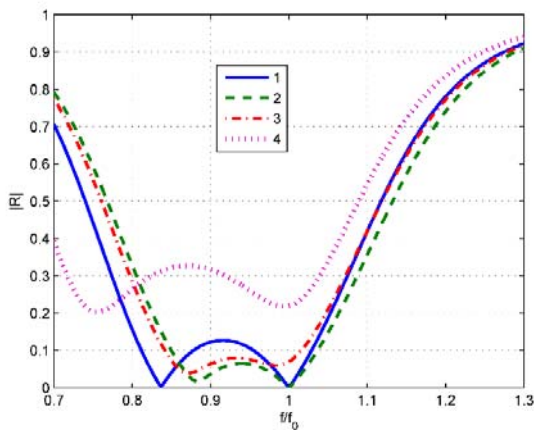


Figure 2. The dependence of the modulus of the reflection coefficient on the frequency, $f_0=f_R$: 1 – bonding layers are taken into account; 2 – bonding layers are not taken into account, and the inductance and capacitance are determined by (13); 3 – bonding layers are taken into account, but the inductance and capacitance are determined by (13); 4 – bonding layers are taken into account, but the inductance and capacitance are $L=1.1L_0$ and $C=C_0$.

The calculation results in Fig. 2 reveal the following significant features.

- 1) The frequency dependence of the modulus of the reflection coefficient is determined by the setting of the LC-elements of the matching circuit (Fig. 1b). Consequently, the reflection coefficient can be tuned after the manufacture of the receiving transducer and the matching circuit, regardless of the technology used and the composition of the layers [22, 23].
- 2) The reflection coefficient can be quite close to zero, $|R|<0.1$, in the acoustic frequency band that is about 15% of

the central frequency (Fig. 2, curve 2). This means that the operating speed of an AO laser Q-switch with active energy extraction in a typical laser resonator remains virtually unchanged compared to a conventional AO laser Q-switch. Thus, for a Q-switch with a central operating frequency of 50 MHz, the modulating frequency band is about 5 MHz (Fig. 2, curve 2), which corresponds to the rise time of the laser pulse front when crossing a typical laser beam with a diameter of 1.0–1.5 mm [14, 15].

Figure 3 shows the frequency dependence of the amplitude U_{inc} of the incident wave and the amplitude $U_{ref}=|R|U_{inc}$ of the reflected wave. The incident wave is a rectangular pulse with a duration of 0.3 μ s with a carrier frequency $f_R=50$ MHz. Frequency dependence of the reflection coefficient $|R|$ corresponds to curve 1 in Fig. 2.

The amplitude U_{ref} of the reflected wave is caused by the diffraction of BAW, and its asymmetry is due to the asymmetry of the frequency dependence of the reflection coefficient with respect to $f=f_0$, see Fig. 2.

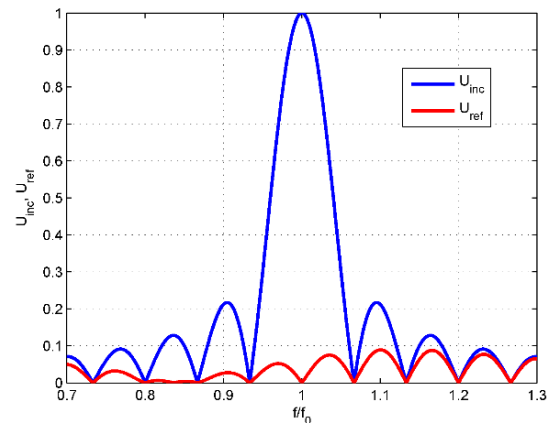


Figure 3. Frequency dependence of the amplitude U_{inc} of the incident wave and the amplitude U_{ref} of the reflected wave. The incident wave is a rectangular pulse with a duration of 0.3 μ s with a carrier frequency $f_R=50$ MHz and $f_0=f_R$.

5. ACOUSTIC RESONATOR WITH FREQUENCY DEPENDENT ACOUSTIC ENERGY REMOVAL

In section 3, theoretical analysis was carried out in the plane wave approximation, revealing that reflection from the crystal-transducer interface is determined by the electrical matching parameters of the piezoelectric transducer with a $R_0=50$ Ohm load (Fig. 1a, b).

Consider the following acoustic structure with two piezoelectric transducers (Fig. 4). The right-hand-side of this structure is the crystal interface corresponding to the structure shown in Fig. 1. The left-hand-side of the structure (Fig. 4): is a mirror image of the right-hand-side. The piezoelectric emitter is supplied with RF power from the generator (the matching circuit of the piezoelectric emitter is not shown). The whole structure is essentially an acoustic resonator, provided that the radiation pattern of the acoustic emitter (left acoustic mirror) coincides with the radiation pattern of the receiver (right mirror). In this case, a necessary condition is a sufficiently high reflection coefficient R from the mirrors. The output of acoustic energy does not occur if the oscillator frequency f lies outside the frequency matching band (Fig. 2, curve 2) $0.85 < f/f_0 < 1.02$, or the matching system of the receiver is turned off. In the matching band of $0.85 < f/f_0 < 1.02$, the acoustic structure loses its resonant properties, the reflection coefficient R from acoustic mirrors decreases, and the structure transforms the energy of acoustic waves into an electrical matched load with minimum losses.

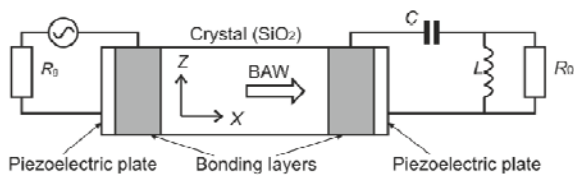


Figure 4. Schematic representation of an acoustic architecture with a piezoelectric emitter (left) and a piezoelectric receiver (right). Left: the output impedance of an amplifier is $R_g=50$ Ohm; right: active resistance of a matched electrical load is $R_0=50$ Ohm.

In practice, it is convenient to measure the admittance of the emitting transducer, and in the RLC circuit of the receiving transducer, L and C are selected so as to minimize (completely eliminate) the beatings of the measured admittance in the vicinity of $f=f_0$. When L and C are properly chosen, the reflection from the receiving transducer reaches a minimum near $f=f_0$, and the admittance beatings caused by the residual standing wave in the resonator are reduced.

6. EXPERIMENT

To verify the theoretical conclusions in this work, an acousto-optic structure based on crystalline quartz SiO_2 with two longitudinal piezoelectric transducers LN 36°YZ

cut was fabricated according to Fig. 4. The orientation of the quartz prism relative to the crystallographic axes corresponded to the known orientation for diffraction of unpolarized laser radiation: a longitudinal acoustic wave propagates along X axis; laser radiation propagates along Z axis (optic axis) of the crystal [19]. Figure 5 shows the custom manufactured experimental acoustic device with matching systems. In terms of its main parameters and functionality, the experimental device fully corresponds to a quartz AO laser Q-switch with a piezoelectric receiver for removing the BAW energy of from the AO element.

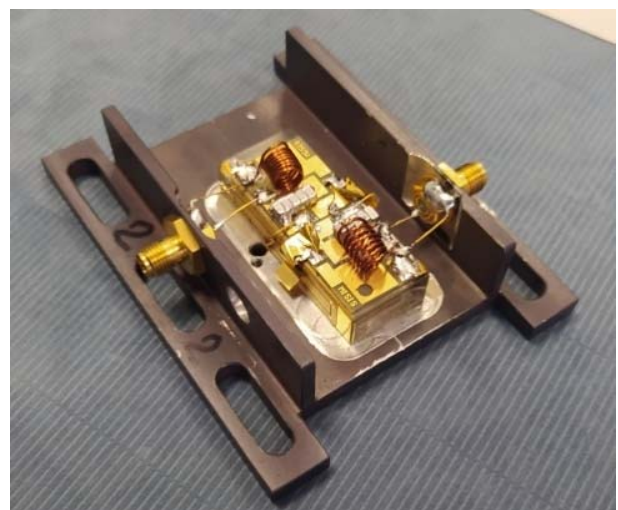


Figure 5. An experimental device for verifying the conclusions of theoretical analysis. Two matching LC circuits are mounted on top of the quartz crystal.

The planes of the piezoelectric emitter and the piezoelectric receiver were parallel. The piezoelectric transducers had identical electrical matching systems, which were tuned in a 50 Ohm circuit using an electrical network analyzer. The central operating frequency of the piezoelectric transducers was 24 MHz. The bandwidth was 21–28 MHz with the standing wave ratio (SWR) less than 1.5.

The fabrication of the piezoelectric transducers was carried out at the Acousto-Optical Research Center, University MISIS, using the original vacuum nanotechnology of solid solutions. The design of the experimental device corresponded to the main goal of the work, i.e., to study the phenomenon of the acoustic energy removal from a crystal under the condition that the acoustic wave is excited in the crystal by an identical piezoelectric transducer.

The magnitude of electrical reflection coefficient from the acoustic structure was measured with a vector electrical network analyzer. This magnitude equals to the modulation

depth of the BAW field owing to standing waves in the crystal. In the experiment, relative modulation depth was below 20% in the matching band of 21–28 MHz. Thus, the AO diffraction efficiency in the Q-switch could be above 80% in the whole frequency bandwidth. For example, the typical value of losses in a completely damped cavity of a Ho^{3+} :YAG laser at $2.1 \mu\text{m}$ is 50% [14], so the residual standing waves in the AO crystal would not result in parasitic lasing in the cavity.

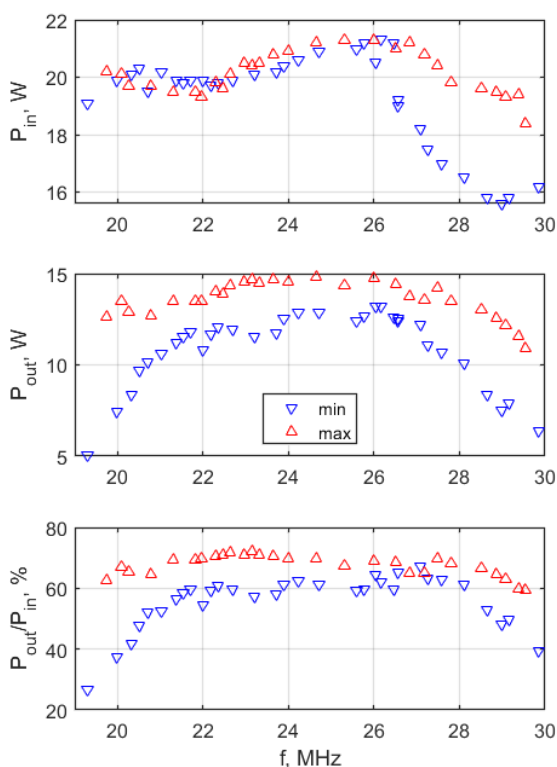


Figure 6. Demonstration of the effect of acoustic energy output from an experimental acoustic structure. In the matching frequency band of 21–28 MHz, the electrical power removed from the crystal is more than 60% of the electrical power supplied to the crystal.

Figure 6 shows the final experimental results of the present study. The plots show the results of measuring the electrical power at the input of the experimental device P_{in} , the electrical power at the output of the device P_{out} , as well as the ratio P_{in} / P_{out} in the frequency range of 20–30 MHz. Red triangles (Δ) correspond to local maxima of the output

power due to standing waves in the acousto-optic crystal; blue triangles (∇) are the local minima. The data were obtained as follows. At a fixed amplitude of the signal supplied from the generator, a local maximum (minimum) of the output power was searched as a function of frequency. The values of the output power, the power entering the acoustic structure, and the standing wave ratio were recorded. The procedure was repeated for a set of maxima and minima in the range of 20–30 MHz. Within the transducers' matching band of 21–28 MHz, the electrical power output from the experimental device is extremely high and ranges from 60 to 70% of the electrical power entering the device at a level of 20 W. Because of small difference in parameters of the transducers and in mutual tuning of the matching circuits of the emitter and receiver, residual standing waves are observed in the crystal affecting the experimental data. In the experiments, it has been also revealed that the acoustic structure is symmetrical: if you swap input and output connectors, almost the same experimental data were obtained.

7. CONCLUSION

The experimental studies of the SiO_2 prototype of the acoustic transmitter-crystal-receiver structure with identical piezoelectric transducers fully confirmed the theoretical conclusions and the usefulness of the practical application of the proposed method for removal the BAW energy from the AO crystal after the interaction. The results of this work allow us to foresee a radical solution to the problem of creating high-power consuming AO devices for the mid-IR range of 2–5 μm .

8. ACKNOWLEDGMENTS

Funding: the research was supported by the Russian Science Foundation (RSF), Project 20-12-00348, <https://rscf.ru/en/project/20-12-00348/>.

9. REFERENCES

- [1] L.N. Magdich and V.Ya. Molchanov: *Acousto-optic Devices and Their Applications*. New York: Gordon and Breach Science Publishers, 1989.
- [2] A. Goutzoulis and D. Pape ed.: *Design and Fabrication of Acousto-Optic Devices*. New York: Marcel Dekker, 1994.

- [3] Molchanov V.Ya., Kitaev Yu.I., Kolesnikov A.I., Narver V.N., Rosenstein A.Z., Solodovnikov N.P., Shapovalenko K.G.: *Theory and practice of modern acousto-optics*. Moscow: MISIS, 2015.
- [4] N.G. Zakharov, O.L. Antipov, V.V. Sharkov and A.P. Savikin: "Efficient lasing at 2.1 μm in a Ho:YAG laser pumped by a Tm:YLF laser," *Quantum Electron.*, vol. 40, no. 2, pp. 98-100, 2010.
- [5] P.A. Ryabochkina, A.N. Chabushkin, N.G. Zakharov, K.V. Vorontsov and S.A. Khrushchalina: "Tunable 2- μm lasing in calcium – niobium – gallium garnet crystals doped with Ho³⁺ ions," *Quantum Electron.*, vol. 47, no. 7, pp. 607-611, 2017.
- [6] A.A. Voronov, V.I. Kozlovskii, Yu.V. Korostelin, A.I. Landman, Yu.P. Podmar'kov, V.G. Polushkin and M.P. Frolov: "Passive Fe²⁺:ZnSe single-crystal Q switch for 3- μm lasers," *Quantum Electron.*, vol. 36, no. 1, pp. 1-2, 2006.
- [7] A.V. Podlipensky, V.G. Shcherbitsky, N.V. Kuleshov, V.P. Mikhailov, V.I. Levchenko, and V.N. Yakimovich: "Cr²⁺:ZnSe and Co²⁺:ZnSe saturable-absorber Q switches for 1.54- μm Er:glass lasers," *Opt. Lett.*, vol. 24, pp. 960-962, 1999.
- [8] V.A. Akimov, V.I. Kozlovskii, Yu.V. Korostelin, A.I. Landman, Yu.P. Podmar'kov, Ya.K. Skasyrskii and M.P. Frolov: "Efficient pulsed Cr²⁺:CdSe laser continuously tunable in the spectral range from 2.26 to 3.61 μm ," *Quantum Electron.*, vol. 38, no. 3, pp. 205-208, 2008.
- [9] V.I. Kozlovskii, Yu.V. Korostelin, A.I. Landman, V.V. Mislavskii, Yu.P. Podmar'kov, Ya.K. Skasyrsky and M.P. Frolov: "Pulsed Fe²⁺:ZnS laser continuously tunable in the wavelength range of 3.49 – 4.65 μm ," *Opt. Lett.*, vol. 41, no. 1, pp. 1-3, 2011.
- [10] J.J. Adams, C. Bibeau, R.H. Page, D.M. Krol, L.H. Furu, S.A. Payne: "4,0-4,5 μm lasing of Fe:ZnSe below 180 K, a new mid-infrared laser material," *Quantum Electron.*, vol. 38, no. 3, pp. 205-208, 2008.
- [11] B.G. Bravy, V.M. Gordienko, V.I. Kozlovsky, Yu.V. Korostelin, F.V. Potemkin, Yu.P. Podmar'kov, A.A. Podshivalov, V.T. Platonenko, V.V. Firsov, M.P. Frolov: "High Power Mid-IR (4–5 μm) Femtosecond Laser System with a Broadband Amplifier Based on Fe²⁺:ZnSe," *Bull. Russ. Acad. Sci. Physics*, vol. 80, no. 4, pp. 444-449, 2016.
- [12] S. Vasilyev, I. Moskalev, M. Mirov, V. Smolski, S. Mirov, V. Gapontsev. "Ultrafast middle-IR lasers and amplifiers based on polycrystalline Cr:ZnS and Cr:ZnSe," *Opt. Mater. Express*, vol. 7, no. 7, pp. 2636-2650, 2017.
- [13] A.V. Pushkin, M.M. Mazur, A.A. Sirotkin, V.V. Firsov, and F.V. Potemkin: "Powerful 3- μm lasers acousto-optically Q-switched with KYW and KGW crystals," *Opt. Lett.*, vol. 44, no. 19, pp. 4837-4850, 2019.
- [14] A.I. Chizhikov, A. V. Mukhin, N.A. Egorov, V.V. Gurov, V.Ya. Molchanov, N.F. Naumenko, K.V. Vorontsov, K.B. Yushkov, and N.G. Zakharov: "High-efficiency KYW acousto-optic Q-switch for a Ho:YAG laser," *Opt. Lett.*, vol. 47, pp. 1085-1088, 2022.
- [15] D. Maydan: "Acoustooptical pulse modulators," *IEEE J. Quantum Electron.*, vol. QE-6, no. 1, p. 15, 1970.
- [16] H. Novotny and E. Benes: "General one-dimensional treatment of the layered piezoelectric resonator with two electrodes," *J. Acoust. Soc. Am.*, vol. 82, pp. 513–521, 1987.
- [17] A.A. Kutsenko, A.L. Shuvalov, O. Poncelet, A.N. Darinskii: "Tunable effective constants of the one-dimensional piezoelectric phononic crystal with internal connected electrodes," *J. Acoust. Soc. Am.*, vol. 137, pp. 606–616, 2015.
- [18] A.N. Darinskii, A.L. Shuvalov, O. Poncelet, A.A. Kutsenko, "Bulk longitudinal wave reflection/transmission in periodic piezoelectric structures with metallized interfaces," *Ultrasonics*, vol. 63, pp. 118-125, 2015.
- [19] US Patent 4,558,926, Dec.17,1985.
- [20] T. Yano, A. Watanabe: "Broad bandwidth acoustooptic devices bonded with thin metal", *IEEE Trans. Son. And Ultrason.*, vol. SU-25, no. 3, pp. 157-159, 1978.
- [21] American Institute of Physics Handbook, American Institute of Physics Eds. Third Ed. McGraw-Hill Book Comp., 1972.
- [22] V.Ya. Molchanov and O.Yu. Makarov: "Phenomenological method for broadband electrical



matching of acousto-optical device piezotransducers,” *Opt. Eng.*, vol. 38, no. 7, pp. 1127-1135, 1999.

- [23] K.B. Yushkov, A.I. Chizhikov, O.Yu . Makarov and V.Ya. Molchanov, “Linear Phase Design of Piezoelectric Transducers for Acousto-Optic Dispersion Delay Lines Using Differential Evolution for Matching Circuit Optimization,” in *IEEE Trans. Ultrason., Ferroelec. Freq. Control*, vol. 67, no. 5, pp. 1040-1047, 2020.

